· Original article ·

Retinal necrosis and apoptosis changes in mice under simulated microgravity

Zhen-Fei Yang[1*], *Wen-Jiong Li*[2*], *Peng Zhang*[2], *Xu Zha*[3], *Xiao Li*[4], *Xiao-Ping Chen*[2], *Si-Quan Zhu*[5]

引用:杨振菲,李文炯,张鹏,等.模拟失重条件下小鼠视网膜坏死和凋亡的变化. 国际眼科杂志 2022;22(11):1765-1770

Foundation item: National Defense Key Laboratory of Science and Technology Fund for Human Factors Engineering (No.6142222180103)

[1]Department of Ophthalmology, Rehabilitation Hospital, National Research Center for Rehabilitation Technical Aids, Beijing 100176, China; [2]State Key Laboratory of Space Medicine Fundamentals and Application, Astronaut Research and Training Center of China, Beijing 100094, China; [3]Department of Ophthalmology, the Second Affiliated Hospital of Kunming Medical University, Kunming 650101, Yunnan Province, China; [4]Department of Ophthalmology, the First Affiliated Hospital of Zhengzhou University, Zhengzhou 450052, Henan Province, China; [5]Department of Ophthalmology, Beijing Anzhen Hospital, Capital Medical University, Beijing 100029, China

Co-first authors: Zhen-Fei Yang and Wen-Jiong Li

Correspondence to: Si-Quan Zhu. Department of Ophthalmology, Beijing Anzhen Hospital, Capital Medical University, Beijing 100029, China. siquanzhu@sina.com; Xiao-Ping Chen. State Key Laboratory of Space Medicine Fundamentals and Application, Astronaut Research and Training Center of China, Beijing 100094, China. xpchen2009@163.com

Received: 2020-05-29 Accepted: 2022-09-29

模拟失重条件下小鼠视网膜坏死和凋亡的变化

杨振菲[1*],李文炯[2*],张 鹏[2],查 旭[3],李 霄[4],陈晓萍[2],朱思泉[5]

基金项目:人因工程国防科技重点实验室基金(No.6142222180103)

作者单位:[1](100176)中国北京市,国家康复辅具研究中心附属康复医院眼科;[2](100094)中国北京市,中国航天员科研训练中心航天医学基础与应用国家重点实验室;[3](650101)中国云南省昆明市,昆明医科大学第二附属医院眼科;[4](450052)中国河南省郑州市,郑州大学第一附属医院眼科;[5](100029)中国北京市,首都医科大学附属北京安贞医院眼科

*:杨振菲与李文炯对本文贡献一致

作者简介:杨振菲,毕业于首都医科大学,博士,主治医师,研究方向:模拟失重状态下视网膜损伤、先天性白内障分子生物学、儿童近视防控;李文炯,毕业于中国航天员科研训练中心,硕士,助理研究员,研究方向:失重生理效应机理与对抗防护研究。

通讯作者:朱思泉,毕业于中山大学,博士,博士研究生导师,主任医师,研究方向:模拟失重状态下视网膜损伤、先天性白内障分子生物学. siquanzhu@sina.com;陈晓萍,毕业于军事医学科学院,博士,博士研究生导师,研究员,研究方向:失重生理效应机理与对抗防护研究. xpchen2009@163.com

摘要

目的:探索模拟失重环境与视网膜损伤的关系。

方法:采用尾吊小鼠试验模拟失重,应用光镜和透射电镜观察视网膜组织形态学变化;应用免疫组织化学和Western blot检测与分析相关的分子变化。

结果:光镜和透射电镜显示:与对照组相比,尾吊组小鼠视网膜神经节层和内核层细胞中均可见更多死亡细胞,相关通路中的TNF-α和caspase-3蛋白表达上调。

结论:在模拟失重环境下小鼠视网膜会产生明显的病理损伤。

关键词:模拟失重;视网膜;TNF-α;;caspase-3;小鼠

Abstract

• AIM: To investigate whether the microgravity environment is related to retinal damage.

• METHODS: Hanging-tail mice tests were used to simulate weightlessness. Light microscopy, and transmission electron microscopic examinations of the retinal tissue structure were used to observe morphological changes. Immunohistochemistry and Western blot analyses were performed to detect the molecular changes associated with the observations.

• RESULT: Light microscopy and transmission electron microscopy demonstrated that more dead cells were detected in the ganglion layer and inner nuclear layer cells. TNF-α and caspase-3 protein expression in the retinas of simulated microgravity groups were up-regulated compared with the ground-based control group.

• CONCLUSION: The results demonstrated that simulated microgravity produced severe pathological damage in the retinas of mice.

• KEYWORDS: simulated microgravity; retina; TNF-α; caspase-3; mice

DOI:10.3980/j.issn.1672-5123.2022.11.01

Citation: Yang ZF, Li WJ, Zhang P, *et al*. Retinal necrosis and apoptosis changes in mice under simulated microgravity. *Guoji Yanke Zazhi* (*Int Eye Sci*) 2022;22(11):1765-1770

INTRODUCTION

With increased interest in human space exploration, the health and safety of space explorers is of foremost concern. Extended spaceflight results in a number of adverse effects, such as bone loss, skeletal muscle atrophy, cardiovascular problems, immune system dysregulation, and eye damage[1-2]. Previous studies have shown that the space environment produced harmful effects on the eye, such as retinal damage (disc edema, globe flattening, choroidal folds, cotton wool spots), cataracts, decreased visual function (decreased near vision, decreased ability to acquire and fixate on the target), and increased intraocular pressure (IOP)[3-4]. Of all known environmental factors in space, including microgravity and ultraviolet and ionizing radiation, microgravity has been recognized as a major factor.

In recent years, the body of evidence has strongly suggested that many human ophthalmic problems occurring during microgravity may be due to cephalad fluid shifts induced by microgravity[5]. Other studies have shown that the changes may result from alterations of the expression of genes and proteins by prolonged exposure to microgravity[6]; however, a comprehensive understanding of the changes to the eye in space and the mechanisms of these changes does not exist. Therefore, it is necessary to evaluate changes to the eye under microgravity conditions and to determine the pathogenesis of the alteration.

The hindlimb unloading (HU) model is widely used to simulate microgravity under laboratory conditions to study the effect of shifting body fluids, which occurs under microgravity conditions[7]. Simulated long-term microgravity can lead to slight IOP fluctuations, choroidal thickening, reduced retinal ganglion cells (RGCs) survival, and optic nerve demyelination in rats[5]. In this study, using the HU model, a set of effects of simulated microgravity (SMG) on retinal cells was analyzed. Mice were exposed to SMG for different time periods to observe the time-dependent effects of SMG exposure. The retinal cells were observed to examine the various responses to SMG, including cell death, mitochondrial swelling, and significant decreases in organelle numbers in the retinal cells[8-10]. TNF-α and caspase-3 protein expressions were each up-regulated in the HU groups, which are related to key molecular events in cell necrosis and apoptosis. To our knowledge, this is the first report to study the retinal changes in mice under SMG conditions.

METHODS

Ethical Approval The study was conducted in accordance to the Declaration of Helsinki. The experimental procedures in mice and the whole protocol used in this study were approved by the Animal Care and Use Committee of China Astronaut Research and Training Center.

Experimental Techniques Eight-week-old male mice (C57BL/6) were obtained from Vital River Laboratories (Beijing, China). The mice were maintained on a standard chow diet at a constant temperature (20°C) under a 12 h/12h artificial light/dark cycle with unlimited access to water. Mice's chow and water were provided ad libitum. The animals were allowed to acclimatize to their new surroundings for 1wk before the study.

To simulate microgravity using the HU model, the body of the mouse makes about a 30° angle from the cage floor, and thus the back feet of the mouse do not touch the grid floor. The mice can move easily and use their front paws without effort. The hind legs should be manually extended to ensure that the toenails do not touch the floor. The angle and height of the mouse were checked and adjusted if necessary on a daily basis. The cage sides were adjustable to increase or decrease the height of the unloading device. The mice must be able to reach food and water after the adjustments are made. The mice were divided to three groups for 0 (the control), 7 (HU7) and 14d (HU14). Each group included eight mice.

Light Microscopy At the end of the experimental treatments, the mice were anesthetized by an intraperitoneal injection of pentobarbital sodium (80 mg/kg). Eyes were collected and fixed in a paraformaldehyde solution (4%). The tissue samples were dehydrated and embedded in paraffin wax. Serial paraffin sections (5μm) were obtained for histological examination. The sections were immersed in xylol for three consecutive washings of 5min to remove paraffin and were subsequently hydrated with five consecutive washings with ethanol in descending order: 100%, 95%, 85%, 75%, and deionized water, respectively. The paraffin sections were then treated with hematoxylin and eosin (HE) staining. Changes in the organizational structure were visualized using light microscopy (LM) (Carl Zeiss Shanghai Co., Ltd. SIP No. MIC01535).

Transmission Electron Microscopy The eyes were cut out of the anterior segment, and the retinas were removed from the posterior segment cup. The retinas were incubated for 4h in 2.5% glutaraldehyde. The retinas were postfixed in buffered osmium tetroxide (1%) and dehydrated using graded solutions of ethanol. Semi-thin sections (1μm) were prepared and stained with toluidine blue, and were examined by visible LM. Ultrathin sections (0.5μm) of the selected areas were prepared and stained with uranyl acetate and lead citrate for TEM (H7650TEM; Hitachi, Tokyo, Japan).

Immunohistochemistry The retinal paraffin tissue sections (5μm) were deparaffinized, and then the histological sections were immersed in a citrate buffer solution and heated at 120℃ in an autoclaved sterilizer for 10min, naturally cooled for 30min, and then they were immersed in 3% aqueous hydrogen peroxide (H_2O_2) for endogenous peroxidase ablation at room temperature for 15min.

The immunohistochemistry for the apoptosis and necrosis markers on the ocular sections was performed using anti-TNF-α, #ab1793, 1∶100 (Abcam, Cambridge, UK) antibody at 4℃ overnight, followed by an anti-mouse IgG

secondary antibody (Beijing ZhongShan Golden Bridge Biotechnology Co., Ltd., Beijing, China) for 2h at room temperature.

The retinal tissues were also treated with the anti-active caspase-3, #ab13847, 1:100 (Abcam, Cambridge, UK) primary antibody at 4℃ overnight, followed by an anti-rabbit IgG secondary antibody (Beijing ZhongShan Golden Bridge Biotechnology Co., Ltd., Beijing, China) for 2h at room temperature.

Finally, the tissue sections were colorated with diaminobenzidine (DAB), kept at room temperature without light for 7min, and then they were counterstained with 2-(4-Amidinophenyl)-6-indolecarbamidine dihydrochloride (DAPI). The positive signals of TNF-α and caspase-3 proteins were a brown or a yellow granular mass.

For the quantitative analysis, the number of TNF-α and caspase-3-positive cells were counted in four fields from each retina section using ImageJ counting plugin 1.41 software (National Institutes of Health, Bethesda, MD). In each retinal region, TNF-α and caspase-3-positive cells were counted in the inner nuclear layer (INL) and ganglion cell layer (GCL). The density profiles were expressed as the mean number of TNF-α and caspase-3-positive cells/mm^2. Similar procedures for density evaluations have been described in the literature. TNF-α and caspase-3-positive cells intensities were averaged across four imaging areas per animal. Statistical analyses were performed using the paired Student's t-test. Differences between groups were considered significant when $P<0.05$.

Protein Expression in the Retina TNF-α protein expression (a key molecular event in cell necrosis and apoptosis) and caspase-3 protein expression (a key molecular event in cell apoptosis) were each examined in the retinas.

The retinas were removed from six mice through a slit in the cornea and were immediately frozen in liquid nitrogen. Retinal protein was extracted with a lysis buffer (Beyotime, Haimen, Jiangsu Province, China) on ice for 30min and was then centrifuged at 15,000r/min at 4℃ for 15min. Protein concentrations were determined using the bicinchoninic acid (BCA) method. An aliquot of the total protein was boiled for 4min, resolved by 10% sodium dodecyl sulfate-polyacrylamide gel electrophoresis (SDS-PAGE), and electrophoretically transferred to polyvinylidene difluoride membranes (Millipore, Darmstadt, Germany). The membranes were blocked with non-fat dry milk in a Tris-buffered saline (5%) containing Tween 20 (0.05%) at room temperature for 1h and were subsequently incubated with mouse monoclonal anti-β-Actin, SC1616, 1:3000 (Santa Cruz Biotechnology, Santa Cruz, California, USA), anti-TNF-α, #3707, 1:500 (Cell Signaling Technology, Boston, Massachusetts, USA), and caspase-3, #9662, 1:1000 (Cell Signaling, Technology, Boston, Massachusetts, USA) antibodies at 4℃ overnight. This procedure was followed by incubation with the appropriate horseradish peroxidase-conjugated secondary antibodies, 1:1000 (Cwbiotech, Beijing, China) at room temperature for 2h. The chemiluminescence reaction was performed using an electrochemiluminescence (ECL) reagent (Thermo Scientific, Waltham, Massachusetts, USA). The blots were scanned and evaluated by densitometry using Quantity One analysis software (Bio-Rad, Hercules, USA), which was normalized for β-Actin density. All experiments were performed in triplicate. The data from the Western blot were evaluated using the paired Student's t-test.

RESULTS

Light Microscopy The results obtained by HE staining demonstrated that hyperpigmented cells with pyknosis (condensation of chromatin in nucleus) were observed in the INL and GCL in the HU7 and HU14 groups. In the retinas of the HU14 group, the pathological damage was observed to be more severe than that in the HU7 group. No obvious pathological changes were found in the retinas of the control group (Figure 1).

Transmission Electron Microscopy Exposure to SMG resulted in changes in the retinal ultrastructure at 1 and 2wk. In both HU groups, the mitochondria in the electron-dense cytoplasm of the cells were swollen. Dead cells were observed in the HU7 group, and the presence of dead cells was determined to be more prevalent in the HU14 group in the GCL. The ganglion cells in the control mice had uniform, normally appearing nuclei and mitochondria; However, vacuolation, chromatin margination, chromatin condensation, and swollen mitochondria were detected in the ganglion cells of both HU groups (Figure 2 A-C). In the inner plexiform layers (IPL), swollen mitochondria were observed in both HU groups (Figure 2 D-F). In the INL, organelles were decreased in number, and dead cells with dark, shriveled nuclei were observed in the HU7 group and were more prevalent in the HU14 group (Figure 2 G-I). No obvious changes were observed in the outer nuclear or retinal pigment epithelium layers. In the control group, no apparent damages were detected in the retinal tissue.

Immunohistochemistry Obvious increases in anti-active caspase-3 expression were observed in the GCL and INL (red arrows) in the HU14 and HU7 retinas compared with the control retinas. Our quantitative assessment revealed that the density of activated TNF-α in the retinal INL and GCL of space-flown mice in the HU7 group was significantly higher (54.5/mm^2) compared to the control group, which had an average of 27.2/mm^2 ($P<0.01$). In the HU14 group, the density of activated TNF-α (106.4/mm^2) increased compared with the HU7 (54.5/mm^2) group ($P<0.01$). Only a sparse positive TNF-α signal was found in sections from ground-control eyes (Figure 3).

A markedly increased number of anti-caspase-3-positive

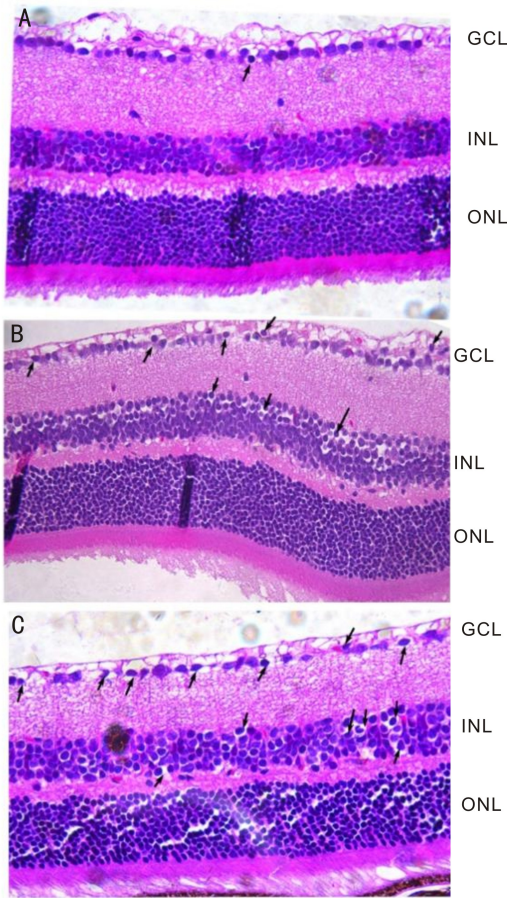

Figure 1 Histopathological analysis of mouse retinas' paraffin sections stained with hematoxylin and eosin. A: the control group (×400); B: the HU7 group (×400); C: the HU14 group (×400). Dead cells (hyperpigmented cells) were increased in ganglion cells and inner nuclear layer cells in the HU7 and HU14 groups (black arrows). GCL: Ganglion cell layer; ONL: Outer nuclear layer; INL: Inner nuclear layer.

granules were visible in the GCL and INL (red arrows) in the HU14 and HU7 retinas compared with the control retinas (Figure 4). As shown in Figure 4, the density profiles in GCL and INL, which reflect the immunoactivity of caspase-3, were significantly increased in the HU7 group at 45.2/mm^2 compared to the control group at 32.1/mm^2 (P<0.01). In the HU14 group, the density of activated TNF-α (106.4/mm^2) increased compared with the HU7 (81.8/mm^2) group (P< 0.01).

Protein Expression in the Retina In the HU7 group, TNF-α protein expression in the retina increased compared with the control group (P < 0.01). In the HU14 group, TNF-α protein expression increased compared with HU7 group (P<0.01; Figure 5).

Caspase-3 protein expression in the retina of the HU7 group was up-regulated compared with the control group (P<0.01). In the HU14 group, caspase-3 protein expression increased compared with the HU7 group (P<0.01; Figure 6).

DISCUSSION

The HU mice model has been widely accepted by the scientific

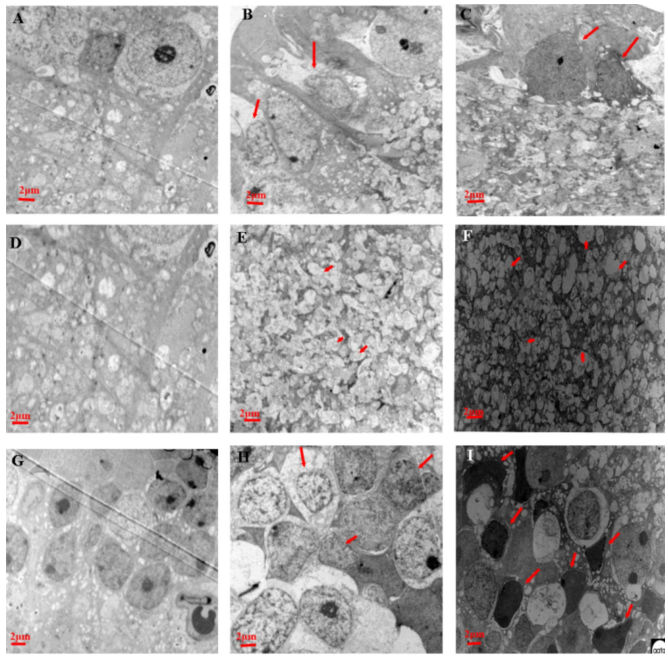

Figure 2 The TEMs of retinal tissue in the control (CON), HU7, and HU14 groups. A: ganglion cell layers of the CON (×7 000); B: ganglion cell layers of the HU7 group (×7000); C: ganglion cell layers of the HU14 group (×7000)—the ganglion cell layers exhibited numerous dead cells (red arrows); D: the inner plexiform layers of the CON (×7000); E: the inner plexiform layers of the HU7 group (×7000); F: the inner plexiform layers of the HU14 group (×7000)—swollen mitochondria were more prevalent in the HU7 and the HU14 groups than in the control group (red arrows); G: the inner nuclear layers of the CON (×7000); H: the inner nuclear layers of the HU7 group (×7000); I: the inner nuclear layers of the HU14 group (×7000)—cells with dark, shriveled nuclei were observed in the HU7 group and were more prevalent in the HU14 group (red arrows).

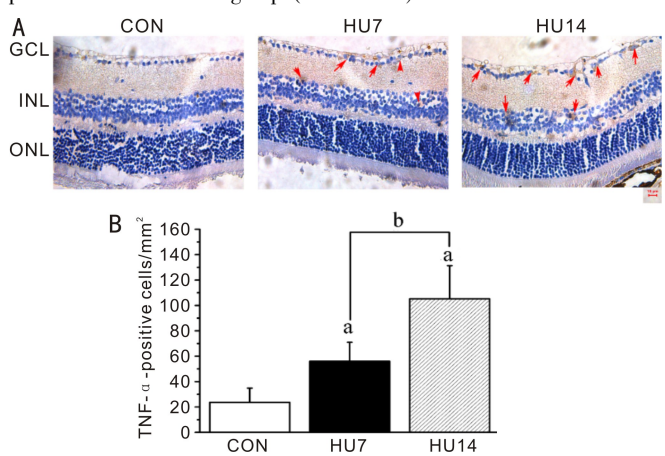

Figure 3 Immunohistochemistry of TNF-α in the retina. A: Representative micrographs of TNF-α immunohistochemical labeling are shown (×400). Cells positive for activated caspase-3 were identified by a brown or yellow granular mass; the nuclei were counterstained with DAPI (blue). Immunoreactivities for TNF-α were present in the ganglion cell layer and inner nuclear layer in the HU7 and HU14 groups (red arrows); only minimally positive staining was detected in the control group. GCL: Ganglion cell layer; ONL: Outer nuclear layer; INL: Inner nuclear layer. B: Quantification of immunoreactivity of TNF-α in retinas. The quantification of TNF-α immunoreactivity is based on the density profile of TNF-α-positive cells in the retinal ganglion cell layer and inner nuclear layer. Bars represent the mean ± SE from three independent experiments. [a]P<0.01 compared with the control group; [b]P<0.01 HU14 compared with the HU7 group.

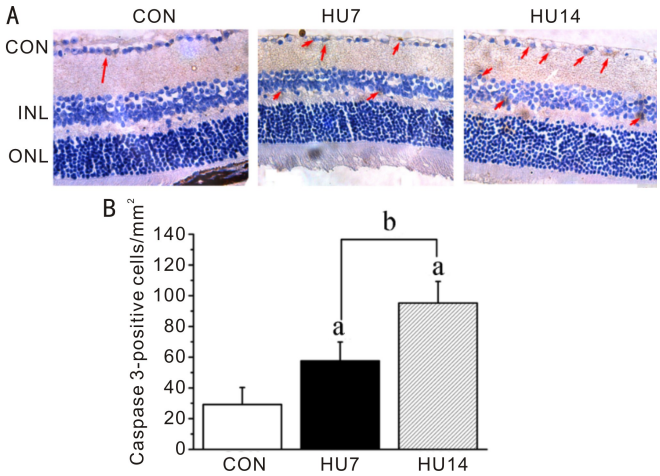

Figure 4 Immunohistochemistry of active caspase-3 in retina. A: Representative micrographs of activated caspase - 3 immunohistochemical labeling are shown (×400). Cells positive for activated caspase-3 were identified by a brown or yellow granular mass; the nuclei were counterstained with DAPI (blue). Immunoreactivities of activated caspase - 3 were present in the ganglion cell layer and inner nuclear layer in the HU7 and HU14 groups (red arrows); only minimally positive staining was detected in the control group. GCL: Ganglion cell layer; ONL: Outer nuclear layer; INL: Inner nuclear layer. Scale bar indicates 10μm. B: Quantification of immunoreactivity of active caspase-3 in retinas. The quantification of active caspase-3 immunoreactivity is based on the density profile of caspase-3-positive cells in the retinal ganglion cell layer and inner nuclear layer. Bars represent the mean ± SE from three independent experiments. [a]$P<0.01$ compared with the control group; [b]$P<0.01$ HU14 compared with the HU7 group.

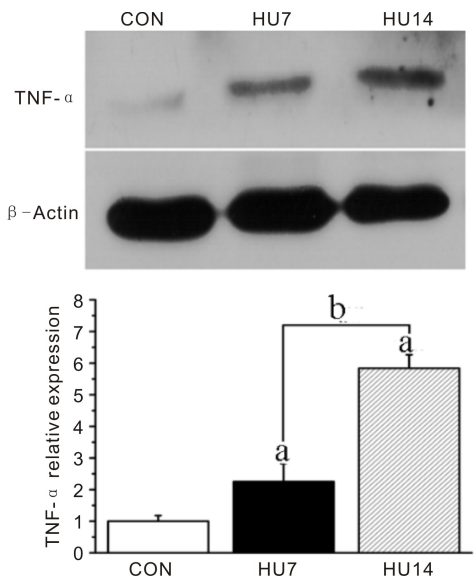

Figure 5 Western blot analysis of TNF-α expression in the retinas of mice. The protein expression of TNF-α was increased in the HU7 group compared to the control group. In the HU14 group, TNF-α protein expression increased compared with the HU7 group. Bars represent the mean ± SE from three independent experiments. [a]$P<0.01$ compared with the control group; [b]$P<0.01$ compared with the HU7 group.

community as the classical model of choice for simulating microgravity[11]. A 30° angle of unloading is recommended because it provides a normal weight bearing on the forelimbs,

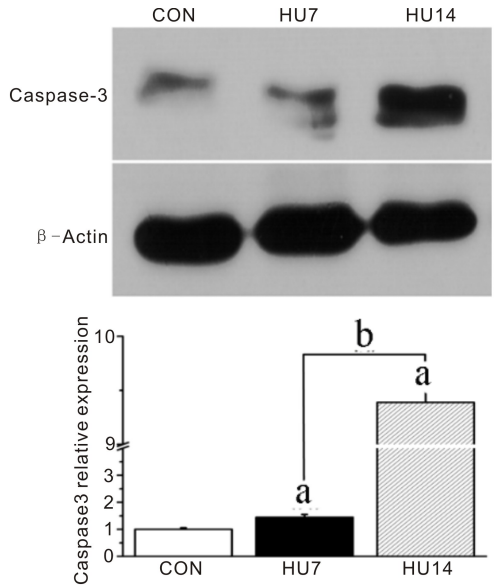

Figure 6 Western blot analysis of caspase-3 expression in the retinas of mice. The protein expression of caspase - 3 was significantly increased in the HU7 group compared to the control group. In the HU14 group, caspase-3 protein expression increased compared with the HU7 group. Bars represent the mean ± SE from three independent experiments. [a]$P<0.01$ compared with the control group; [b]$P<0.01$ compared with the HU7 group.

unloads the lumbar vertebrae but not the cervical vertebrae, and induces a cephalad fluid shift[12]. Data which used the model showed differential muscle atrophy and a cephalad fluid shift, so the HU model was initially designed to study musculoskeletal, cardiovascular. The HU mice model was useful for investigating the responses of many other physiological systems to unloading and the recovery from unloading on earth.

With the current state of technological development, people can remain in space for longer periods of time. Several studies have demonstrated that visual function is influenced by a weightless environment. In 2011, Mader *et al*[1] conducted ophthalmic examinations on seven astronauts after 6mo of space flight and reported observations consisting of cotton wool spots, disc edema, choroidal folds, globe flattening and nerve fiber layer thickening. The research confirmed that microgravity can cause cell apoptosis[13]. At the cellular level, retinal ganglion cells survival was reduced, optic nerve oligodendrocytes were reduced, and microglia - mediated inflammation - related factors and apoptotic factors were discovered in both optic nerve and the retina[5].

In the present investigation, the HU model was designed to simulate the weightless condition in mice. The results demonstrated retinal pathological changes occurred, such as the degeneration and necrosis of retinal cells. The injuries associated with 14d of microgravity were severer compared to the microgravity conditions for a period of 7d. Some of the pathological changes were not reversible and could affect retinal function. Therefore, precautions and the mechanisms for such effects must be investigated to protect retinal damage in astronauts.

The retinal changes during exposure to microgravity may have caused cephalad fluid shifts that induced increases in intracranial and vein pressure. Increased intracranial pressure is directly transmitted from the intracranial compartment to the intraorbital compartment through the subarachnoid space[12]. The trans-lamina cribrosa pressure difference results in axonal swelling of the optic nerve and visible disc edema. Elevated SAS pressure and a swollen optic nerve are believed to exert force on the central retinal artery, which supplies blood to the five inner layers of the retina, resulting in retinal ischemia and leading to cell death. In addition, the increased vortex vein pressure may cause decreased choroidal drainage and may lead to blood pooling of the choroid. This process could result in an increase in choroidal volume and may account for the rise in IOP. The thickening choroidal fluid and increased IOP could have resulted in the extrusion of the retina. This force causes retinal ischemia, which may lead to retinal cell death. Previous research has shown that gene expression can alter in the space environment[14]. Some of the changes may constitute an adaptation in the space environment, but some changes may damage organisms. In the present study, TNF-α protein levels were elevated in the retina following SMG. TNF-α is known to affect cell necrosis or apoptosis (two distinct modes of cell death), growth, differentiation and survival. TNF-α also plays an important role in various intraocular diseases, such as uveitis, glaucoma, retinal degeneration and retinal ischemia. The increased expression of TNF-α in the retina may be related to retinal injury. The caspase enzymes play vital roles in the induction, transduction and amplification of intracellular apoptotic signals[15]. Caspase-3, one of the most important caspase enzymes, is considered to be the effector and executioner of apoptosis. The data generated in this research demonstrated that SMG conditions up-regulated the activity of caspase-3 in the retina, which suggests that caspase-3 is involved in SMG-induced cell death in the retina.

In conclusion, SMG conditions in mice resulted in retinal injury. The TNF-α and caspase-3 signaling pathways were activated in retinal cells following exposure to SMG conditions. The results indicated that the TNF-α and caspase-3 signaling pathways may be interesting targets to protect retinal cells from apoptosis/necrosis following SMG.

The ophthalmology health of astronauts is closely related to human spaceflight. Long-term microgravity exposure can lead to spaceflight-associated neuroocular syndrome, which can present with optic disk edema, globe flattening, choroidal folds and a hyperopic visual shift. So this study used hanging-tail mice tests to simulate weightlessness. SMG conditions in mice resulted in retinal injury. The results indicated that the TNF-α and caspase-3 signaling pathways may be interesting targets to protect retinal cells from apoptosis/necrosis following SMG. The results provide a certain help for the research on astronauts' eye damage in a weightless environment.

REFERENCES

1 Mader TH, Gibson CR, Pass AF, *et al*. Optic disc edema, globe flattening, choroidal folds, and hyperopic shifts observed in astronauts after long-duration space flight. *Ophthalmology* 2011; 118(10): 2058-2069

2 Taibbi G, Cromwell RL, Kapoor KG, Godley BF, Vizzeri G. The effect of microgravity on ocular structures and visual function: a review. *Surv Ophthalmol* 2013;58(2):155-163

3 Özelbaykal B, Öğretmenoğlu G, Tunçez IH. Ocular Outcomes in Healthy Subjects Undergoing a Short-Term Head-Down Tilt Test. *Aerosp Med Hum Perform* 2021; 92(8):619-626

4 Laurie SS, Macias BR, Dunn JT, Young M, Stern C, Lee SMC, Stenger MB. Optic disc edema after 30 days of strict head-down tilt bed rest. *Ophthalmology* 2019;126(3):467-468

5 Li SQ, Song QY, Wu B, Kan GH, Wang F, Yang JW, Zhu SQ. Structural damage to the rat eye following long-term simulated weightlessness. *Exp Eye Res* 2022;223:109200

6 Shimada N, Sokunbi G, Moorman SJ. Changes in gravitational force affect gene expression in developing organ systems at different developmental times. *BMC Dev Biol* 2005;5:10

7 Morey-Holton ER, Globus RK. Hindlimb unloading rodent model: technical aspects. *J Appl Physiol* (1985) 2002;92(4):1367-1377

8 Schulz H, Strauch SM, Richter P, Wehland M, Krüger M, Sahana J, Corydon TJ, Wise P, Baran R, Lebert M, Grimm D. Latest knowledge about changes in the proteome in microgravity. *Expert Rev Proteomics* 2022;19(1):43-59

9 Strauch SM, Grimm D, Corydon TJ, Krüger M, Bauer J, Lebert M, Wise P, Infanger M, Richter P. Current knowledge about the impact of microgravity on the proteome. *Expert Rev Proteomics* 2019;16(1):5-16

10 Zhao HW, Shi YY, Qiu CY, Zhao J, Gong YB, Nie C, Wu B, Yang YY, Wang F, Luo L. Effects of simulated microgravity on ultrastructure and apoptosis of choroidal vascular endothelial cells. *Front Physiol* 2021; 11:577325

11 Dai XF, Ye SM, Chen XP, Jiang T, Huang HX, Li WJ, Yu HQ, Bao JH, Chen H. Rodent retinal microcirculation and visual electrophysiology following simulated microgravity. *Exp Eye Res* 2020; 194:108023

12 Salerni F, Repetto R, Harris A, Pinsky P, Prud'homme C, Szopos M, Guidoboni G. Biofluid modeling of the coupled eye-brain system and insights into simulated microgravity conditions. *PLoS One* 2019; 14(8):e0216012

13 Prasad B, Grimm D, Strauch SM, Erzinger GS, Corydon TJ, Lebert M, Magnusson NE, Infanger M, Richter P, Krüger M. Influence of microgravity on apoptosis in cells, tissues, and other systems *in vivo* and *in vitro*. *Int J Mol Sci* 2020;21(24):9373

14 Mao XW, Pecaut MJ, Stodieck LS, Ferguson VL, Bateman TA, Bouxsein M, Jones TA, Moldovan M, Cunningham CE, Chieu J, Gridley DS. Spaceflight environment induces mitochondrial oxidative damage in ocular tissue. *Radiat Res* 2013;180(4):340-350

15 Chen G, Gong M, Yan M, Zhang XM. Sevoflurane induces endoplasmic reticulum stress mediated apoptosis in hippocampal neurons of aging rats. *PLoS One* 2013;8(2):e57870